Molecular Microbiology (2010) 77(3), 743–754 ■
doi:10.1111/j.1365-2958.2010.07245.x
First published online 15 June 2010

Metabolic shutdown in *Escherichia coli* cells lacking the outer membrane channel TolC

Girija Dhamdhere and Helen I. Zgurskaya*
Department of Chemistry and Biochemistry, University of Oklahoma, 620 Parrington Oval, Room 208, Norman, OK 73019, USA.

Summary

The outer membrane channel TolC is a key component of multidrug efflux and type I secretion transporters in *Escherichia coli*. Mutational inactivation of TolC renders cells highly susceptible to antibiotics and leads to defects in secretion of protein toxins. Despite impairment of various transport functions, no growth defects were reported in cells lacking TolC. Unexpectedly, we found that the loss of TolC notably impairs cell division and growth in minimal glucose medium. The TolC-dependent phenotype was further exacerbated by the loss of *ygiB* and *ygiC* genes expressed in the same operon as *tolC* and their homologues *yjfM* and *yjfC* located elsewhere on the chromosome. Our results show that this growth deficiency is caused by depletion of the critical metabolite NAD^+ and high $NADH/NAD^+$ ratios. The increased amounts of PspA and decreased rates of NADH oxidation in Δ*tolC* membranes indicated stress on the membrane and dissipation of a proton motive force. We conclude that inactivation of TolC triggers metabolic shutdown in *E. coli* cells grown in minimal glucose medium. The Δ*tolC* phenotype is partially rescued by YgiBC and YjfMC, which have parallel functions independent from TolC.

Introduction

TolC is the universal outer membrane portal for export of toxins and drug efflux in *Enterobacteriacea* species (Andersen *et al*., 2001). Previous studies showed that *Escherichia coli* cells lacking *tolC* are highly susceptible to multiple antibiotics and fail to secrete microcin J25, colicin V, haemolysin and heat-stable enterotoxin II (Gilson *et al*., 1990; Holland *et al*., 1990; Yamanaka *et al*., 2008). TolC was also found to be involved in cysteine tolerance, as well as in secretion of porphyrins and enterobactin (Bleuel *et al*., 2005; Cosme *et al*., 2008; Tatsumi and Wachi, 2008; Wiriyathanawudhiwong *et al*., 2009). More recently, TolC-deficient cells were shown to overproduce MarA, SoxR and Rob transcriptional regulators (Rosner and Martin, 2009). This finding suggested that TolC might be involved in extrusion of metabolites. In many human pathogens, TolC is required for host invasion but specific substrates secreted within hosts remain unknown (Ferhat *et al*., 2009; Platz *et al*., 2009; Webber *et al*., 2009).

The diverse functionality of TolC is based on its ability to interact with multiple transporters and their accessory proteins located in the inner membrane and the periplasm (Tikhonova *et al*., 2009; Zgurskaya, 2009). When assembled, the TolC-dependent transport complexes are believed to span the entire envelope of *E. coli* and expel their substrates from the cytoplasm or the periplasm into the external medium. Some of these complexes, such as type I secretion systems, are assembled only transiently when the substrate is ready to be translocated across the outer membrane (Thanabalu *et al*., 1998). In contrast, the constitutively produced multidrug transporters exemplified by AcrAB form more stable associations with TolC that are independent from the presence of substrates (Tikhonova and Zgurskaya, 2004; Touze *et al*., 2004).

In the genome of *E. coli* and other enterobacteria, the chromosomal *tolC* locus contains three genes *tolC*, *ygiB* and *ygiC*, which are presumably expressed in a single operon (Fig. 1A). However, functions of YgiB and YgiC as well as any functional link between these proteins and TolC remain unknown. Sequence analyses identified YgiB as an outer membrane lipoprotein containing a putative type II signal peptide. YgiB is highly conserved in cyanobacteria and proteobacteria but its homologues are also present in some Gram-positive species where they precede the *ygiC*-like genes.

YgiC shares significant homology with the C-terminal domain of *E. coli* GspS, a bifunctional enzyme possessing both glutathionylspermidine (GSP) synthetase and GSP amidase activities (Bollinger *et al*., 1995). The C-terminal domain of GspS is a GSP synthetase belonging to the ATP-Grasp ATPases family of proteins, which also include the human glutathione (GSH) synthetase (Pai *et al*., 2006). The high conservation of catalytically important residues in YgiC suggested that this protein could be a GSP synthetase.

Accepted 26 May, 2010. *For correspondence. E-mail elenaz@ou.edu; Tel. (+1) 405 325 1678; Fax (+1) 405 325 6111.

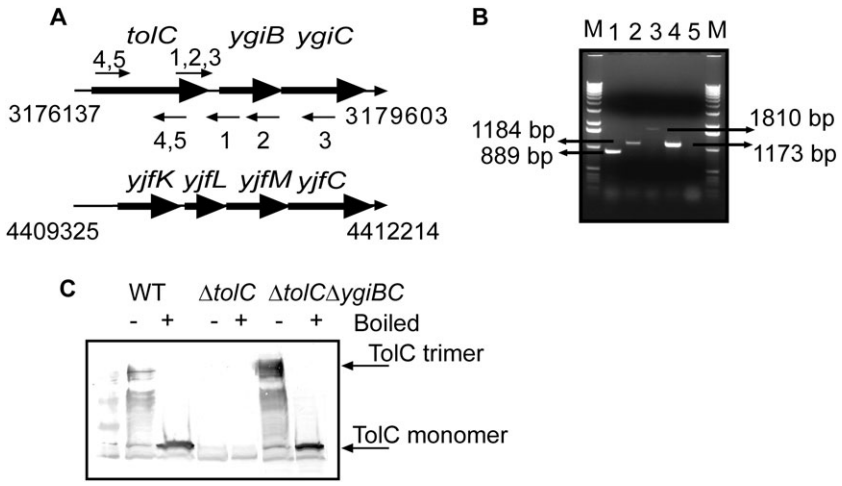

Fig. 1. TolC is expressed in a single operon with *ygiBC*.
A. Structures of *tolC-ygiBC* and *yjfKLMC* operons. Annealing regions of primers used in reverse transcriptase (RT)-PCR reactions are indicated as small arrows.
B. RT-PCR analysis of RNA isolated from *E. coli* BW25113 (WT) strain. The same RNA sample was used in all reactions. Lanes 1–3: RT-PCR reactions with forward and reverse primers that anneal to *tolC-ygiB* transcript (primers 1, 2 and 3 in A). Lane 4: RT-PCR reaction using forward and reverse primers that anneal to *tolC* transcript (primers 4, 5 in A). Lane 5 is the same reaction as in lane 4 but RT was omitted (no DNA control).
C. Immunoblotting analysis of TolC in WT (BW25113), Δ*tolC* (GD100) and Δ*ygiBC* (GD101) cells. Twenty micrograms of total membrane proteins were separated on 12% SDS-PA gel. TolC was visualized using polyclonal anti-TolC antibody.

The GSP conjugate was initially detected in *E. coli* under stationary or anaerobic growth conditions (Tabor and Tabor, 1975). Subsequently GSP was identified in parasites as a precursor of trypanothione, a critical redox-active, thiol-containing biomolecule (Fairlamb *et al*., 1986). The physiological function of bacterial GSP however is unclear and *E. coli* cells lacking GspS synthetase do not have any phenotype under laboratory conditions (Bollinger *et al*., 1995). In agreement with this observation, mutants that do not produce either GSH or spermidine (SPE), the two constituents of GSP, also lack growth phenotype, presumably because thioredoxins and other polyamines can replace GSH and SPE in their numerous functions (Tabor *et al*., 1978; Xie *et al*., 1993; Fuchs, 1995).

In this study, we investigated how the lack of TolC impacts cell physiology and discovered a functional link between YgiBC/YjfMC and TolC. We report that inactivation of TolC causes stress in the inner membrane. The membrane stress leads to metabolic shutdown, inhibition of NADH dehydrogenases and growth arrest. The function of YgiBC/YjfMC partially protects membranes from the damage and enables ΔTolC cells to grow in the minimal medium with glucose.

Results

tolC *mRNA contains* ygiB *and* ygiC *sequences*

To confirm that *tolC* is transcribed as a part of an operon we performed reverse transcriptase (RT)-PCR analysis of RNA isolated from *E. coli* BW25113 cells [wild type (WT)]. Figure 1B shows that primers complementary to *tolC* and either to *ygiB* or to *ygiC* regions amplify the expected products only when reverse transcriptase is present in the reaction mixture. Thus, all three *tolC*, *ygiB* and *ygiC* genes are transcribed together.

We next tested whether *ygiBC* genes are involved in regulation of TolC expression or assembly. Immunoblotting analysis with anti-TolC antibody detected no changes in TolC levels or trimerization in the absence of *ygiBC* (Fig. 1C). This result implied that *ygiBC* products are not required for the post-transcriptional expression of TolC.

TolC-dependent growth defect of ΔygiBCΔyjfMC *mutant*

The arrangement in a single operon suggested that functions of YgiB and YgiC could be linked to that of TolC. Therefore, we investigated growth phenotypes of cells lacking *tolC* alone, *ygiBC* alone or the entire operon. Consistent with previous results, no defects were found when *tolC* mutant (GD100) was grown in Luria–Bertani (LB) broth (Fig. 2A). In the minimal M9 medium however GD100 cells delayed exiting from the stationary phase for at least 4 h and in the exponential phase grew 30% slower than the WT cells. The *E. coli* mutant with the deletion of the entire *tolC-ygiBC* operon (GD102) was phenotypically similar to Δ*tolC* (Table 1).

The BLAST analysis showed that *E. coli* chromosome contains two genes *yjfM and yjfC* homologous to *ygiB* and

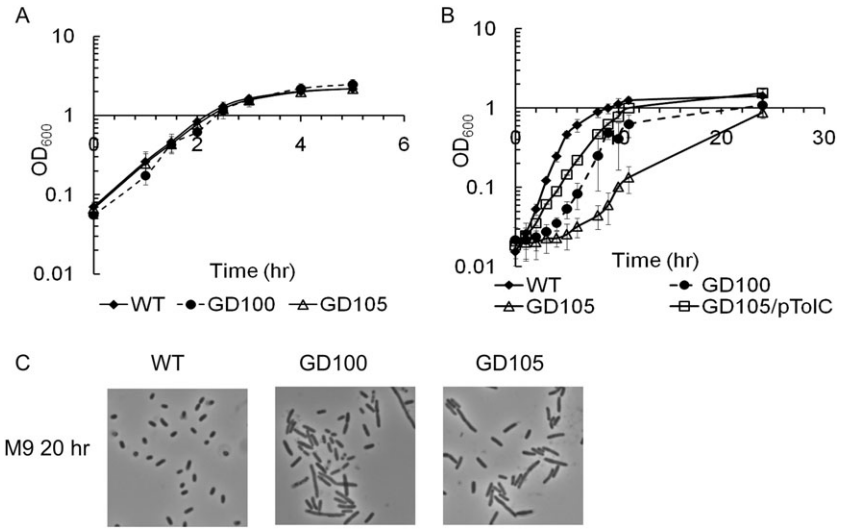

Fig. 2. Growth and cell division defects of Δ*tolC* cells.
A and B. Overnight cultures of WT, GD100 (Δ*tolC*) and GD105 (Δ*tolC-ygiBC* Δ*yjfMC*) grown either in LB (A) or in M9 (B) were re-inoculated (1:100) into the fresh matching medium. The growth was monitored by measuring absorbance at 600 nm. The initial cell densities were adjusted to approximately the same value. For each growth curve the average of three independent experiments is shown. Error bars are standard deviations (SD, $n = 3$).
C. Phase-contrast microscopy. Cells were grown overnight in LB, diluted 1:100 into fresh M9 medium and incubated at 37°C for 20 h.

ygiC respectively. The *yjfM* gene shares 23% identity and 40% similarity with *ygiB*, whereas *yjfC* and *ygiC* are 50% identical. The *yjfMC* genes are preceded by two additional genes of unknown functions, which together with *yjfMC* form an *yjfKLMC* operon (Fig. 1A). Since *yjfMC* are highly homologous to *ygiBC*, functions of these two sets of genes could be complementary to each other. Therefore, we constructed Δ*tolC* mutants containing deletions in *yjfMC* alone (GD111) and in both *ygiBC* and *yjfMC* (GD105). Similar to Δ*tolC* and Δ*tolC-ygiBC* strains, the LB grown GD111 had the WT phenotype, but in M9 these cells experienced a 2 h lag when exiting the stationary phase and grew slower than the WT (Table 1). This growth deficiency phenotype was significantly exacerbated in GD105 cells. Upon re-inoculation into a fresh M9 medium (M9-to-M9), the overnight-grown GD105 cells experienced approximately 8 h of lag time and once resumed, the growth rate was only half of the WT (0.34 ± 0.1 h^{-1}, Table 1). Therefore, the deletion of either YgiBC or YjfMC alone does not further compromise the Δ*tolC* phenotype. However, when both gene sets are deleted, Δ*tolC* cells have significant growth defects in M9. This result suggested that YgiBC and YjfMC have complementary functions that enable growth of Δ*tolC* cells in M9.

Reciprocally, the growth phenotype of Δ*ygiBC*Δ*yjfMC* cells depended on TolC. The TolC$^+$ cells lacking *ygiBC* and *yjfMC* (GD104) had the WT phenotype in both LB and M9 media (Table 1). Furthermore, the growth phenotype of GD105 cells was rescued by the plasmid carrying *tolC* alone (Fig. 2B). Taken together these results suggest that

Table 1. Growth rates of *E. coli* mutants in LB and minimal M9 media (h^{-1}).

Name	Genotype[a]	LB	M9 (lag time, h)
BW25113	WT	1.22 ± 0.13	0.62 ± 0.05
GD100	*ΔtolC*	1.12 ± 0.08	**0.44 ± 0.05**[b] **(4 ± 1.8)**
GD101	*ΔygiBC*	1.14 ± 0.18	0.63 ± 0.01
GD102	*ΔtolC-ygiBC*	1.04 ± 0.003	**0.55 ± 0.05 (5.3 ± 0.6)**
GD103	*ΔyjfMC*	1.17 ± 0.04	0.63 ± 0.02
GD104	*ΔygiBC ΔyjfMC::kan*	1.03 ± 0.01	0.65 ± 0.03
GD105	*ΔtolC-ygiBC ΔyjfMC::kan*	1.11 ± 0.03	**0.34 ± 0.10 (7.8 ± 1.7)**
GD111	*ΔtolC::kan ΔyjfMC*	1.01 ± 0.007	**0.43 ± 0.08 (1.3 ± 0.5)**
JW0117-1	*ΔspeE::kan*	ND	0.52 ± 0.04
JW2914-1	*ΔgshB::kan*	ND	0.57 ± 0.04
JW2956-1	*ΔgspS::kan*	ND	0.55 ± 0.04
JW2663-1	*ΔgshA::kan*	ND	0.58
GD106	*ΔspeE ΔtolC::kan*	ND	**0.49 ± 0.06 (1.8 ± 0.6)**
GD107	*ΔgshB ΔtolC::kan*	ND	**0.52 ± 0.06 (3 ± 1.4)**
GD108	*ΔygiBC ΔyjfMC ΔgspS::kan*	ND	0.58 ± 0.03
GD109	*ΔspeE ΔygiBC::kan*	ND	0.61 ± 0.02

a. Positions of kanamycin cassette when applicable are indicated.
b. Here and in all other tables, values in bold are significantly different from the BW25113 strain.
Averages of three independent experiments and standard deviations are shown.
ND, no data.

Table 2. Susceptibility of *E. coli* strains to antimicrobial agents.

Strain	Genotype	ERY	NOV	NOR	SDS
BW25113	WT	32	32	0.04	10 240
ETBW	*ΔtolC*	**1**	**1**	**0.01**	**5**
GD101	*ΔygiBC*	64	128	0.04	10 240
GD102	*ΔtolC-ygiBC*	1	1	0.01	5
GD103	*ΔyjfMC*	64	64	0.04	10 240
GD104	*ΔygiBC ΔyjfMC::kan*	64	128	0.04	10 240
GD105	*ΔtolC-ygiBC ΔyjfMC::kan*	**1**	**0.25**	**0.005**	**5**

Numbers are minimal inhibitory concentrations, MICs, in μg ml^{-1}. All experiments were repeated at least three times.
ERY, erythromycin; NOV, novobiocin; NOR, norfloxacin; SDS, sodium dodecyl sulphate.

TolC and YgiBC/YjfMC have parallel, independent functions. When both functions are compromised *E. coli* is unable to grow efficiently in the minimal medium.

Determination of colony-forming units and the LIVE/DEAD BacLight staining of cells showed that in stasis and during extended lags Δ*tolC* cells are viable. For all strains, we found that the number of dead cells is less than 5% and remains the same in the exponential and stationary phases. However, GD100 and GD105 cells when grown in M9 were notably longer than the WT indicating cell division defects (Fig. 2C).

GD105 cells are more susceptible to antibiotics

To investigate whether inactivation of *ygiBC* and/or *yjfMC* affects antibiotic susceptibility of *E. coli* cells we measured minimal inhibitory concentrations (MICs) of antibiotics erythromycin, novobiocin and norfloxacin and detergent SDS (Table 2). Consistent with previous studies, Δ*tolC* cells were highly susceptible to all tested compounds. However, deletions of either *ygiBC* or *yjfMC*, alone and in combination, in the WT and Δ*tolC* backgrounds did not increased susceptibility to antibiotics. The only notable change was the two- to fourfold decrease of MICs of novobiocin and norfloxacin in GD105 (Δ*tolC-ygiBC* Δ*yjfMC*). We conclude that *ygiBC* and/or *yjfMC* do not contribute to intrinsic levels of antibiotic resistance but their absence aggravates the Δ*tolC* phenotype.

ΔtolC *cells are depleted of essential metabolites*

To investigate why Δ*tolC* cells have problems growing in M9, we measured concentrations of NAD^+ and NADH during the LB-to-M9 transition and in the stationary phase. NAD^+ and NADH are the major players in microbial metabolism and their absolute and relative amounts report on the metabolic and redox states of cells (Gennis and Stewart, 1996). Consistent with their growth phenotypes, the NAD^+ concentrations were at the same ≈1.5 mM levels in WT and mutants growing in LB (Table 3). After transition into stationary phase, the concentration of NAD^+ decreased in all strains but GD105 cells contained the lowest 0.3 mM NAD^+.

Table 3. NAD^+ and NADH concentrations in exponential and stationary-phase cells.

		LB		M9		
Strains		1 h	12 h	1 h	12 h	20 h
BW25113	NAD^+, mM	1.4 ± 0.28	0.77 ± 0.29	1.5 ± 0.06	1.1 ± 0.15	0.78 ± 0.29
	NADH, mM	0.48 ± 0.2	0.21 ± 0.06	0.38 ± 0.13	0.63 ± 0.08	0.61 ± 0.27
	$NADH/NAD^+$	0.3	0.3	0.2	0.5	0.8
GD104	NAD^+, mM	1.7 ± 0.03	0.43 ± 0.01	1.5 ± 0.1	1.1 ± 0.14	0.52 ± 0.007
	NADH, mM	0.97 ± 0.04	0.21 ± 0.07	0.25 ± 0.07	0.5 ± 0.007	0.36 ± 0.01
	$NADH/NAD^+$	0.6	0.5	0.2	0.4	0.7
GD100	NAD^+, mM	1.2 ± 0.3	0.79 ± 0.2	1.4 ± 0.08	1.1 ± 0.01	**0.34 ± 0.01**
	NADH, mM	0.80 ± 0.4	0.19 ± 0.06	0.5 ± 0.09	0.4 ± 0.06	0.35 ± 0.06
	$NADH/NAD^+$	0.7	0.2	0.4	0.4	1.0
GD105	NAD^+, mM	1.35 ± 0.18	**0.29 ± 0.2**	1.57 ± 0.3	**0.47 ± 0.04**	**0.08 ± 0.02**
	NADH, mM	0.94 ± 0.47	**0.34 ± 0.18**	0.36 ± 0.06	**0.29 ± 0.01**	**0.23 ± 0.01**
	$NADH/NAD^+$	0.7	**1.2**	0.2	0.6	**2.9**
GD105/pTolC	NAD^+, mM	1.51 ± 0.01	0.52 ± 0.05	1.2 ± 0.1	0.99 ± 0.01	0.6 ± 0.05
	NADH, mM	1.1 ± 0.01	0.26 ± 0.05	0.3 ± 0.003	0.51 ± 0.06	0.51 ± 0.01
	$NADH/NAD^+$	0.7	0.5	0.3	0.5	0.8

All strains contained similar concentrations of NAD^+ and NADH 1 h after the shift into M9 medium (Table 3). However, transition into the stationary phase caused a significant drop of NAD^+ concentration in GD105. Extension of stasis for 20 h led to further decrease of NAD^+ to 0.08 mM in GD105 cells and the threefold drop to 0.3 mM of NAD^+ in GD100. Thus, when growing in M9, albeit to a different degree, GD100 and GD105 cannot efficiently synthesize NAD^+. This leads to dilution and eventual depletion of this critical cofactor in the stationary phase.

Interestingly, WT and Δ*tolC* mutants also responded differently to stasis in terms of concentration of NADH. Although amounts of NADH increased in the M9 12 and 20 h samples of the WT cells reflecting the reduced respiration and starvation, the amounts of this cofactor did not change significantly in GD100 and GD105 cells. As a result, despite the large difference in absolute concentrations, the NADH/NAD^+ ratio was close to one in the M9 20 h samples of WT and GD100 but increased to almost three in GD105 cells due to dramatic depletion of NAD^+. This result strongly suggests that in M9 medium, GD105 is not only deficient in biosynthetic activities but cannot oxidize NADH as well.

The NAD^+ depletion in stationary GD105 cells was rescued by a plasmid carrying *tolC* alone suggesting that expression of TolC is required and sufficient to maintain normal metabolism in M9 medium (Table 3). In agreement, GD104 cells, which are $TolC^+$ but lack *ygiBC* and *yjfMC*, contained normal NADH/NAD^+ ratios.

Taken together these results show that inactivation of TolC causes depletion of essential metabolites when cells enter stasis. The depletion of NAD^+ is notably accelerated in GD105 cells and in minimal medium. The unusually high NADH/NAD^+ ratio and low concentrations of NAD^+ imply that stationary GD105 cells are in the state of the metabolic shutdown.

NADH dehydrogenases are inhibited in ΔtolC *cells*

During aerobic metabolism, the major pool of NADH is re-oxidized on the membrane by two membrane-bound NADH dehydrogenases NDH-I and NDH-II (Yun *et al.*, 2005). Thus, either one or both of these proteins could be inhibited in GD105 cells. Therefore, we next measured the NADH oxidase activity in membrane fractions isolated from WT and Δ*tolC* mutants grown in LB and M9 media. We found that exponential WT and mutant cells contained similar levels of the membrane-bound NADH oxidase activity (Table 4). Consistent with previous reports this activity did not depend on the growth medium and was the same for the LB and M9 grown cells (Dancey *et al.*, 1976). In the stationary WT and GD100 cells, the NADH oxidase activity decreased by 25–35%. In contrast, the NADH oxidase activity of GD105 membranes dropped two- to threefold when cells entered stasis in either medium and was 40–60% lower than in the stationary WT cells. Thus, in accord with NADH/NAD^+ measurements (Table 3), GD105 membranes cannot efficiently oxidize NADH. We conclude that inhibition of membrane-bound NADH dehydrogenases contributes to metabolic shutdown in Δ*tolC* cells.

Table 4. Specific NADH oxidase activity of WT and Δ*tolC* membranes.

Medium, time of incubation	BW25113	GD100	GD105
	NADH oxidase activity (U mg^{-1})		
LB, 1 h	0.39 ± 0.06	0.46 ± 0.09	0.39 ± 0.03
LB, 12 h	0.28 ± 0.02	0.28 ± 0.04	**0.13 ± 0.01**
M9, 1 h	0.49 ± 0.09	0.33 ± 0.04	0.52 ± 0.1
M9, 12 h	0.31 ± 0.1	0.36 ± 0.05	**0.21 ± 0.01**
M9, 20 h	0.35 ± 0.007	**0.24 ± 0.07**	**0.20 ± 0.05**

Deletion of TolC creates stress in the inner membrane

To investigate how Δ*tolC* cells respond to metabolic shutdown, we compared protein profiles of cytoplasmic and membrane fractions isolated from exponential and stationary-phase cells. Protein compositions of the exponential WT and Δ*tolC* mutant cells were very similar. However, upon transition into the stationary-phase Δ*tolC* cells significantly overproduced a 26 kDa membrane protein (Fig. 3). No major changes in protein composition were found in GD104 cells lacking only *ygiBC/yjfMC* (data not shown). The 26 kDa protein from Δ*tolC* membranes was readily solubilized with 1% sarcosyl indicating that the protein is associated with the inner membrane. The N-terminal protein sequencing identified this protein as a phage shock protein A, PspA. PspA is a peripheral inner membrane protein, which is induced specifically by membrane stress and dissipation of a proton motive force (PMF) (Kobayashi *et al.*, 2007). Thus, inactivation of TolC creates stress on the cytoplasmic membrane of *E. coli*.

Growth defects of GD105 cells are suppressed by L*-serine*

The experiments described above established that the membrane stress and metabolic shutdown in GD100 and GD105 cells are aggravated in the M9 medium, whereas LB medium suppresses these defects. This result suggested that certain nutrients or vitamins might alleviate the problems these cells experience in M9. Indeed, the growth rate and rapid exit from stasis of GD105 strain was restored by supplementing M9 medium with 0.4% casamino acids (Fig. 4A).

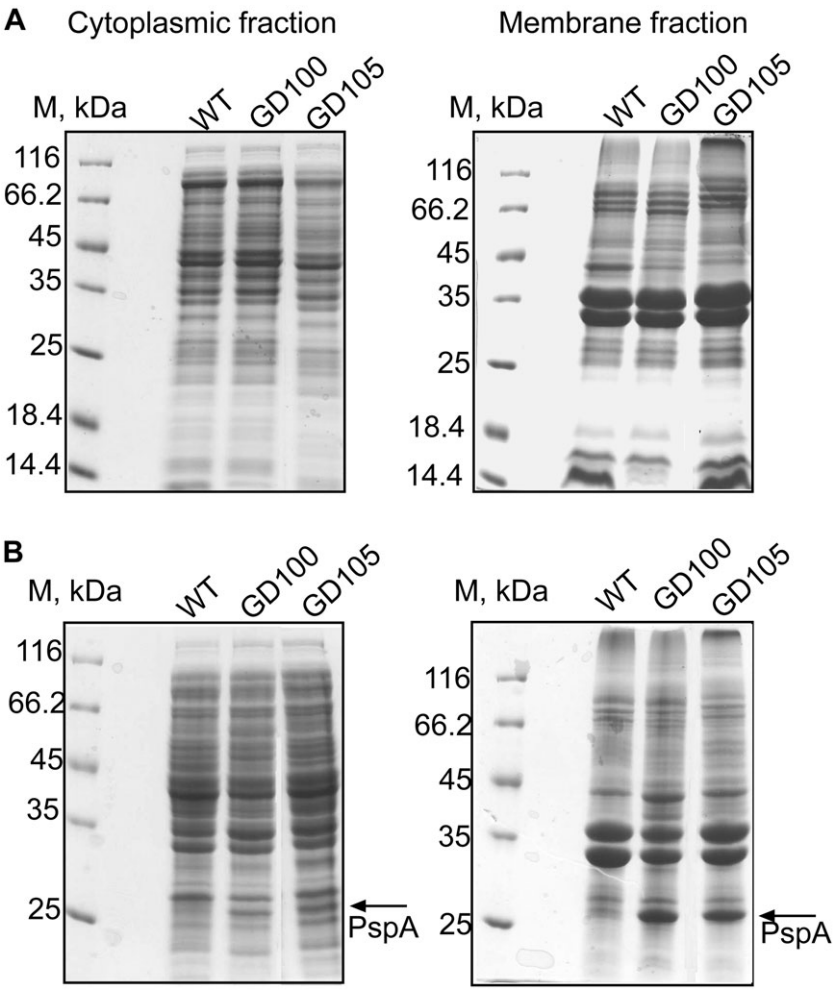

Fig. 3. Stationary-phase Δ*tolC* cells overproduce the membrane stress protein PspA. SDS-PAGE analysis of the cytoplasmic and membrane fractions isolated from the exponential (A) and stationary (B) cultures of WT and Δ*tolC* mutants.

We next tested various vitamins and amino acids for their ability to restore normal growth of GD105 in M9. Among six tested amino acids only L-serine restored completely the growth phenotypes of these cells to that of the WT (Fig. 4A). Although glycine and cysteine are synthesized from L-serine, neither of these two amino acids could restore the GD105 growth in M9. Furthermore, consistent with previous reports (Wiriyathanawudhiwong *et al.*, 2009), we found that cysteine inhibits the growth of all Δ*tolC* mutants (data not shown). Thus, in M9 medium Δ*tolC* and GD105 cells became auxotrophic for L-serine.

Interestingly, despite the normal growth in the M9 medium supplemented with L-serine, the stationary-phase

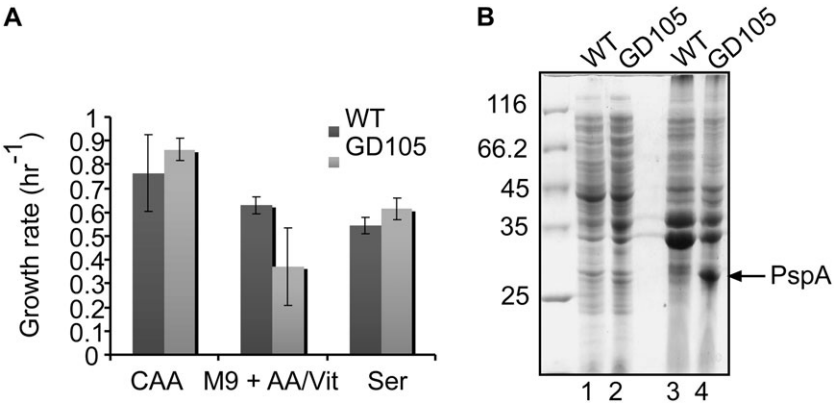

Fig. 4. Growth defects, but not the membrane stress of GD105 cells, are rescued by L-serine.
A. Growth rates of WT and GD105 cells in M9 supplemented with casamino acids, individual amino acids or vitamins.
B. SDS-PAGE analysis of the cytoplasmic (lanes 1 and 2) and membrane (lanes 3 and 4) fractions isolated from the stationary (48 h) cultures of WT and GD105.

Δ*tolC* cells still contained the elevated amounts of PspA protein (Fig. 4B). We conclude that L-serine supplementation does not prevent membrane stress caused by the inactivation of TolC but likely enables cells to repair membranes and resume growth in the presence of glucose.

Cells lacking glutathione, spermidine and glutathionylspermidine do not have the TolC-dependent growth defect

In all assays described above, deletions of *ygiBC* and *yjfMC* significantly aggravated the metabolic problems of the stationary-phase Δ*tolC* cells. Since YgiC/YjfC and GspS share significant homology, all three proteins might be involved in synthesis of GSP. Furthermore, previous studies suggested that GSP accumulates in the stationary-phase *E. coli* cells (Smith *et al*., 1995). To investigate whether the lack of GSP contributes to growth defects of GD105, we constructed *E. coli* cells lacking all three GSP synthetases: *gspS*, *ygiC* and *yjfC* (GD108). However, GD108 cells had the WT phenotype when growing in M9 (Table 1). Thus, the lack of GSP alone does not cause growth defects in M9.

To further investigate the putative functional link between GSP synthetases and TolC we constructed Δ*tolC* mutants that are also deficient in the synthesis of either GSH (Δ*gshB* and Δ*gshA* mutants lacking GSH synthetase and γ-glutamate-cysteine ligase respectively) or SPE (Δ*speE* lacking spermidine synthase). Previous studies confirmed that these mutants do not produce GSH and SPE respectively (Xie *et al*., 1993; Fuchs, 1995). We found however that these cells grow in M9 medium with the same rate as Δ*tolC* cells (Table 1). Furthermore, double Δ*gshB*Δ*speE* mutant producing neither GSH nor SPE does not have any significant growth defect in M9 medium. These results strongly suggested that metabolic defects of GD100 and GD105 are not linked to the biosynthetic pathways of GSH, SPE or GSP.

ΔtolC *cells deplete glutathione*

Earlier studies suggested that both GSH and GSP are expelled from the *E. coli* and *Salmonella* stationary cells (Smith *et al*., 1995). To investigate whether inactivation of TolC in GD100 and GD105 strains leads to accumulation of these metabolites, we compared the amounts and composition of non-protein thiols in cells grown either in LB or M9 medium. As a negative control, we used Δ*gshA* cells, which do not produce GSH and its precursor γ-Glu-Cys (Helbig *et al*., 2008).

We first determined whether there is any change in the composition of the reduced thiols. For this purpose, intracellular thiols were derivatized with monobromobimane (MBB) and analysed by HPLC (Fairlamb *et al*., 1986). Figure 5 shows that the composition of non-protein thiols is identical in the WT and Δ*tolC* mutants growing in LB, with the major peak identified as GSH. Although previous studies suggested that GSH is converted into GSP upon transition into the stationary phase (Tabor and Tabor, 1975; Smith *et al*., 1995), we did not find larger amounts of GSP in the stationary-phase cells (Fig. 5). When incubated in M9, the major difference between the WT and Δ*tolC* cells was a significant decrease in the amounts of GSH in GD105 cells even 1 h after the shift into M9 (M9 1 h). Furthermore, 20 h of incubation in M9 (M9 20 h) led to the drop of GSH amounts below detection limits in both GD100 and GD105 cells (Fig. 5C and D).

To quantify GSH and its oxidized form glutathione disulphide (GSSG) we used the glutathione reductase assay (Anderson, 1985). In agreement with HPLC data, 1 h after LB-to-M9 shift, GD100 maintained [GSH+GSSG] at levels similar to those in the WT but the amounts of [GSH+GSSG] decreased more than eightfold to ≈1.8 mM in the stationary M9 20 h cells (Table 5). The depletion of GSH was accelerated in GD105 cells. These cells lost half of their [GSH+GSSG] 1 h after transfer into M9 and were down to 0.3 mM of [GSH+GSSG] in the stationary phase (M9 20 h). Thus, similar to NAD^+/NADH, the amounts of GSH are rapidly depleted when Δ*tolC* mutants enter the stationary phase in M9. The concentrations of GSSG were extremely low in all cells (less than 1 μM, data not shown) indicating that the dramatic drop of GSH concentration in stationary GD100 and GD105 cells was not caused by its oxidation.

Micromolar concentrations of GSH were detected in supernatants of all stationary-phase cultures except Δ*gshA* cells that do not produce GSH (Table 5). Interestingly, despite lower intracellular GSH levels and lack of TolC, GD100 and GD105 cells excreted up to 10 times more GSH than the WT cells, with GD105 releasing the largest amounts of GSH. Thus, TolC is not required for GSH efflux. Furthermore, the higher concentrations of GSH in supernatants suggest that Δ*tolC* cells leak GSH into medium.

Discussion

In this study, we found that TolC-deficient *E. coli* cells are defective when grown in minimal medium with glucose. The growth defect manifests itself in the decreased growth rate, the prolonged lag when exiting the stationary-phase and altered morphology. This phenotype is further exacerbated by the lack of *ygiBC* and *yjfMC* gene products, which share homology with GSP synthetases. Based on the results presented here and extant literature we propose that stress on the cytoplasmic membrane and inhibition of NADH dehydrogenases are the major causes of the TolC-dependent growth defects.

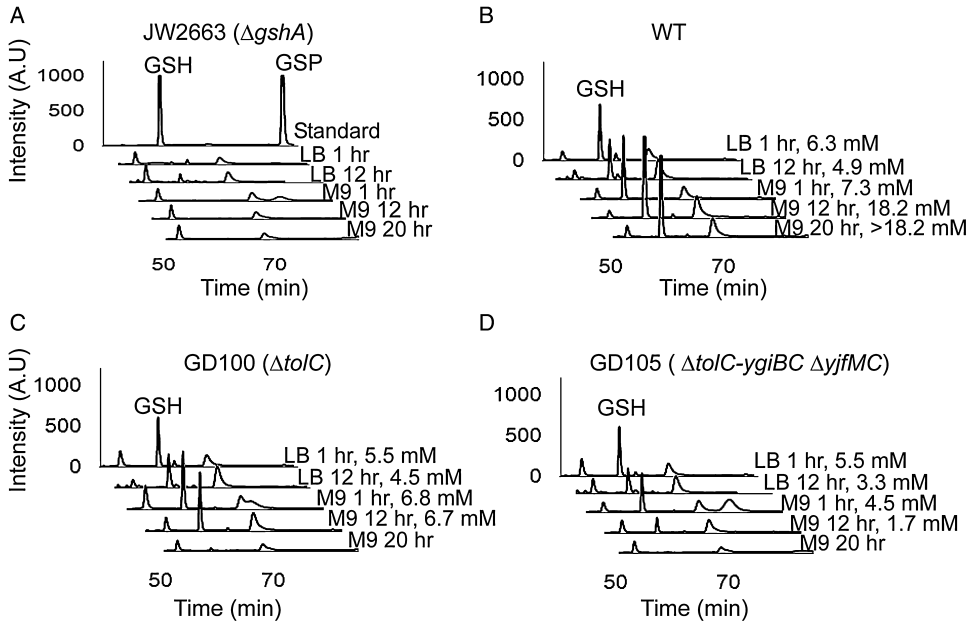

Fig. 5. The M9 grown Δ*tolC* cells deplete endogenous GSH. Exponentially growing WT and mutant cells were collected by centrifugation, washed and re-suspended either in LB or in M9 medium. At indicated time points, intracellular non-protein thiols were derivatized with MBB and separated by HPLC.
A. Top lane, GSH and GSP standards derivatized with MBB; bottom lanes, MBB-labelled thiols from Δ*gshA* cells.
B–D. MBB-labelled non-protein thiols from the WT, GD100 and GD105 respectively. The intracellular concentrations of GSH when detectable were calculated from peak area using the calibration curve generated with GSH. These are indicated for each profile where GSH is detectable.

We found that membrane fractions of the stationary Δ*tolC* cells contain large amounts of PspA (Fig. 3). PspA is known to be overproduced in response to various extracytoplasmic challenges such as osmotic shock, misfolded membrane proteins or presence of ionophore CCCP (Kleerebezem *et al*., 1996). A well-established commonality among various Psp-activating signals is reduction in the membrane electrochemical potential, which drives the PMF. Therefore, membranes of the Δ*tolC* cells are under the stress that dissipates PMF. This stress is most profound when Δ*tolC* cells enter the stationary phase (Table 3, Fig. 3). The stationary phase in general is stressful to *E. coli* as evidenced by activation of various stress response systems in starving cells (Nystrom, 2004). Furthermore, one of the most damaging starvation-induced stresses is oxidative stress (Dukan and Nystrom, 1999). Interestingly, recent study reported that cells lacking TolC overproduce stress response proteins SoxS, MarA and Rob (Rosner and Martin, 2009). Among these factors, SoxRS regulon is known to specifically respond to the intracellular accumulation of superoxide. Thus, Δ*tolC* cells cannot efficiently detoxify this oxygen derivative, which could further aggravate the oxidative stress in starving cells.

In addition to membrane stress, Δ*tolC* cells are severely depleted in essential metabolites. The decrease of GSH concentration in GD105 is notable already 1 h after transfer into M9 medium (Fig. 5 and Table 5).

Table 5. Intracellular (in) and excreted (out) concentrations of glutathione in the WT and Δ*tolC* mutants.

	BW25113		GD100		GD105	
	GSH+GSSG, mM		GSH+GSSG, mM		GSH+GSSG, mM	
Medium, time of incubation	in	out	in	out	in	out
LB, 1 h	10.4 ± 0.1	ND	9.7 ± 0.8	ND	7.6 ± 1.9	ND
LB, 12 h	8.1 ± 0.4	ND	8.3 ± 0.01	ND	7.8 ± 1.2	ND
M9, 1 h	8.8 ± 0.7	–	7.1 ± 0.3	–	**4.2 ± 0.3**	–
M9, 12 h	17.7 ± 1.9	0.001 ± 0.002	**8.5 ± 0.1**	**0.008 ± 0.0003**	**2.4 ± 0.2**	**0.009 ± 0.001**
M9, 20 h	15.1 ± 0.6	0.019 ± 0.001	**1.8 ± 0.5**	**0.014 ± 0.001**	**0.3 ± 0.1**	**0.005 ± 0.0004**

ND, no data; –, below detection levels.

However, it is in the stationary phase the concentrations of both GSH and NAD^+ become very low in both GD100 and GD105 cells (Tables 3 and 5). The degree of metabolite depletion correlates with the time required for these two mutants to exit the stasis and resume growth in the fresh medium. GD105 cells cannot resume the growth for up to 8 h after transfer into a fresh medium, whereas GD100 start growing after 2–4 h of delay (Fig. 2). Since the number of live cells is the same in WT and Δ*tolC* cells, we suggest that Δ*tolC* cells cannot exit the stasis because of the stress on the membrane and low concentration of NAD^+ but resume growth when they replenish depleted metabolites and repair the membranes.

Growth of Δ*tolC* cells is also significantly hindered by abnormal NADH/NAD^+ ratios. In the stationary GD105 cells the concentration of NADH exceeds that of NAD^+ almost three times (Table 3) and this problem is serious in both LB and M9 media. For comparison, shift under anaerobic conditions leads to change in the NADH/NAD^+ ratios in *E. coli* cells from 0.2 to only 0.67 (Leonardo *et al.*, 1996). High levels of NADH impact *E. coli* physiology on several levels. First, large NADH/NAD^+ ratios inhibit key enzymes, e.g. citrate synthase and malate dehydrogenase, shared by the tricarboxylic acid cycle (TCA) and the glyoxylate shunt (Pruss *et al.*, 1994). Therefore, in GD105 these metabolic pathways are disabled and these cells cannot efficiently catabolize or synthesize metabolites that require the TCA cycle.

Second, high concentrations of NADH despite the drop in amounts of NAD^+ indicate that activity of NADH dehydrogenases is inhibited as well. Indeed, we found that rates of NADH oxidation in GD105 membranes decrease significantly upon entry into stasis and remain only at 50% level of the WT (Table 4). NADH oxidation in *E. coli* is carried out by multiple enzymes (Gennis and Stewart, 1996). However, previous studies showed that mutational inactivation of the membrane-bound NADH dehydrogenase NDH-I leads to growth defects during transition into the stationary phase (Pruss *et al.*, 1994). These defects of NDH-I mutants can be suppressed by serine. Similarly, we found that serine suppresses the growth defects of Δ*tolC* cells (Fig. 4). In addition, NDH-I couples NADH oxidation to production of a PMF. The overproduction of PspA in Δ*tolC* membranes indicates a decrease in a PMF. Taken together these findings suggest that TolC inactivation leads to inhibition of NDH-I, which in turn results in metabolic shutdown and dissipation of a PMF.

Finally, NADH acts as an iron reductant in a Fenton reaction and drives DNA damage by iron and peroxide *in vivo* (Brumaghim *et al.*, 2003). Previous studies showed that raising the NADH level *in vivo* by eliminating or negatively regulating NADH dehydrogenase activity dramatically sensitizes *E. coli* to killing by peroxide (Imlay and Linn, 1988). Thus, high levels of NADH in GD105 cells could contribute significantly to oxidative stress in these cells. We suggest that rising levels of NADH are the major reasons for the induction of SoxS, MarA and Rob stress responses in the cells lacking TolC.

It remains unclear whether inactivation of one specific TolC-dependent function or a cumulative effect of the loss of multiple transport activities is responsible for the membrane stress and growth phenotypes of Δ*tolC* cells. It is often assumed that diverse phenotypes of Δ*tolC* cells are caused by accumulation of toxic metabolites or by the lack of secretion (Rosner and Martin, 2009; Wiriyathanawudhiwong *et al.*, 2009). We found however that cells lacking the major drug efflux pump AcrAB and its homologue AcrEF have the WT phenotype (data not shown). Our results suggest that stress on the cytoplasmic membrane and metabolic defects in Δ*tolC* cells, rather than loss of efflux, contribute significantly to most of the previously reported phenotypes.

All Δ*tolC* phenotypes are significantly aggravated by the lack of YgiBC and YjfMC proteins. YgiC and YjfM share highly conserved catalytic residues with GspS and are likely to conjugate GSH and spermidine in the cytoplasm. However, their counterparts YgiB and YjfM are peripheral membrane proteins located in the periplasm. The function of GSP and YgiBC and YjfMC proteins are unknown. Our studies suggest that activities of these proteins are not dependent on the GSH and spermidine biosynthetic pathways (Table 1) but are needed for protection of the inner membrane. We noticed that the PspA-like transcriptional regulator is located immediately upstream of the *yjfKLMC* operon, further strengthening the notion that the function of these proteins might be related to the maintenance or protection of the cytoplasmic membrane.

Experimental procedures

Strains and plasmids

All *E. coli* strains constructed in this study are derivatives of BW25113 (*lacI*^{q} *rrnB*$_{T14}$ Δ*lacZ*$_{WJ16}$ *hsdR514* Δ*araBAD*$_{AH33}$ ΔΔ*rhaBAD*$_{LD78}$) (Datsenko and Wanner, 2000). The BW25113 derivatives JW0117-1 (Δ*speE*), JW2914-1 (Δ*gshB*), JW2956-1 (Δ*gspS*), JW2663 (Δ*gshA*) were obtained from the Keio collection (distributed by *Coli* Genetic Stock Center at Yale University) and confirmed with PCR. All mutants were constructed using λ red recombinase system and antibiotic resistance genes were removed as described in Datsenko and Wanner (2000). The genotypes of strains and positions of antibiotic resistance cassettes, when appropriate, are indicated in Table 1. All gene disruptions including purchased strains were confirmed with PCR. The plasmid pTolC carrying *tolC* under IPTG-inducible P_{tac} promoter was a gift from Dr Rajeev Misra.

Growth media and conditions

Cells were grown in a rotary shaker set at 220 r.p.m. and 37°C either in LB broth (10 g of Bacto tryptone, 10 g of yeast extract and 5 g of NaCl per litre) or in M9 minimal medium [5 × M9 salts (Difco), 0.4% glucose, 2 mM $MgSO_4$ and 0.1 mM $CaCl_2$]. Growth rates were measured after 1:100 dilution of the overnight grown cultures into fresh LB or M9 media. The sequential second and third re-inoculation into M9 medium showed that the GD105 phenotype is stable and that resumption of the growth is not caused by suppressor mutants. Changes in cell density were monitored by measuring absorbance at 600 nm. Growth rates were calculated from the linear slopes of the logarithmic plots of growth curves. *P*-values were calculated using Microsoft Office Excel and were found to be 0.011 and 0.010 for GD100 and GD105 respectively. To determine the amino acid requirements, strains were grown in M9 medium supplemented with either 0.4% casamino acids or one of the following amino acids: 0.2 g l^{-1} L-aspartic acid, 0.6 g l^{-1} L-glutamic acid, 0.1 g l^{-1} L-serine, 0.2 g l^{-1} L-methionine, 0.2 g l^{-1} L-glycine, 0.1 g l^{-1} L-cysteine.

Minimal inhibitory concentrations

Minimal inhibitory concentrations of various antimicrobial agents were measured in 96-well plates (Tikhonova *et al*., 2002). Approximately 10^4 exponentially growing cells were inoculated in LB medium supplemented with twofold increasing concentrations of antibiotic. Plates were incubated overnight at 37°C without shaking.

Reverse transcriptase-PCR

Reverse transcriptase-PCR was performed by using QIAGEN OneStep RT-PCR kit. Total RNA was isolated from exponentially growing cells (LB broth) using QIAGEN RNeasy kit. Two micrograms of purified total RNA were used for RT-PCR. To detect the *tolC* transcript (reaction 4 in Fig. 1), the forward primer 5′-AATGCAAATGAAGAAATTGC and the reverse primer 5′-CGCGTACCGACGCAGTAGCCCGCTTC were used to yield a product of 1173 bp. To detect the *ygiB* and *ygiC* mRNA (reactions 1, 2 and 3 on Fig. 1) the forward primer 5′-CAAAGCTCATTATGCGCGATGGAAGCG and the reverse primers (1) 5′-CATCATGTAACCGGCCATCAG-3′, (2) 5′-GATGTAGAGGAACTCAGTAGC-3′ and (3) 5′-GTATC AGCCACCCATTGAACG-3′ were used to yield products of 889 bp, 1184 bp and 1810 bp respectively.

Protein expression profiles

Wild type and mutants grown overnight in M9 were diluted 1:100 into fresh M9 medium and incubated at 37°C with shaking at 220 r.p.m. Cells were collected by centrifugation in the exponential phase (OD_{600} = 0.6) and 48 h after inoculation into the fresh medium. Cells were then washed and re-suspended in the buffer containing 10 mM Tris-HCl (pH 8.0) and 5 mM EDTA and then treated with 100 μg ml^{-1} lysozyme for 40 min. Sonication was used to lyse cells. Unbroken cells were removed by low speed centrifugation and membranes were collected by ultracentrifugation for 1 h at 100 000 *g*. Membrane pellets were re-suspended in buffer containing 50 mM Tris-HCl (pH 8.0), 100 mM NaCl and 1 mM PMSF. The cytoplasmic and membrane fractions [20 μg of total protein as estimated using Bradford assay with bovine serum albumin (BSA) as a standard] in the SDS sample buffer were boiled for 5 min and then analysed using standard 12% SDS-PAGE and Coomassie Brilliant Blue staining.

NAD^+ and NADH measurements

NADH recycling assay was used to determine intracellular concentrations of NAD^+ and NADH (Matsumura and Miyachi, 1980). Cells growing in LB (OD_{600} ~ 1.0) were collected by centrifugation and either re-suspended in the same volume of fresh LB or washed and then re-suspended in fresh M9. Cells were incubated at 37°C with shaking (220 r.p.m.) and were collected by centrifugation at 1, 12 and 20 h post re-inoculation. For the assay, ~5×10^9 cells were collected by centrifugation at 15 700 *g* for 2 min, the cell pellets were frozen in dry ice ethanol bath and stored at –80°C until use. A total of 250 μl of 0.2 M NaOH (for NADH extraction) or 250 μl of 0.2 M HCl (for NAD^+ extraction) was added to the frozen pellets, samples were boiled for 10 min and then centrifuged at 9300 *g* for 5 min. The NAD^+ and NADH supernatants were immediately used for assay.

The reaction mixture contained 30 μl of 1.0 M BICINE-NaOH (pH 8.0), 75 μl of cell extract, 75 μl of 0.1 M NaOH for NAD^+ samples or 0.1 M HCl for NADH samples, 30 μl of 16.6 mM phenazine ethosulphate, 30 μl of 4.2 mM 3-[4,5-dimethylthiazol-2-yl]-2,5-diphenyltetrazolium bromide (MTT), 30 μl of absolute ethanol and 30 μl of 40 mM EDTA (pH 8.0). The reaction mix was pre-incubated for 3 min at room temperature and 6 μl of 500 U ml^{-1} yeast alcohol dehydrogenase enzyme was added to start the reaction. The rate of reduction of MTT, which is directly proportional to amounts of NAD^+ and NADH in samples, was monitored at 570 nm for 5 min. Standard curves were generated by using 0.125–1.25 nmol of NAD^+ and NADH (Sigma) respectively.

NADH oxidase assay

Cell membrane preparations and the NADH oxidase assay were performed as described before (Osborn *et al*., 1972; Tikhonova and Zgurskaya, 2004). Briefly, cells were incubated in LB and M9 media for 1, 12 and 20 h as described above. Spheroplasts were prepared by EDTA-lysozyme treatment. After sonication, unbroken cells were removed by low-speed centrifugation and membranes were collected by ultracentrifugation for 1 h at 100 000 *g*. Membrane pellet was re-suspended in 10 mM Tris-HCl (pH 8.0), 0.25 M sucrose. Protein concentration of membranes was measured using Bradford assay with BSA as a standard. Fifty micrograms of total protein was used for the assay. The assay mixture contained 50 mM Tris-HCl (pH 7.5), 0.3 mM DTT and 0.60 μM NADH (Sigma). Rate of decrease in absorbance at 340 nm was measured for 1 min.

Determination of GSP, GSH and GSSG content

Two methods were used to determine the composition and concentration of non-protein thiols. HPLC was used to analyse intracellular thiols derivatized with MBB as described in Fairlamb *et al*. (1986) and Helbig *et al*. (2008). Cells were incubated in LB and M9 media for 1, 12 and 20 h as described above. A total of 1×10^9 cells (1.0 OD_{600}) were washed with fresh M9 medium and re-suspended in buffer containing 40 mM HEPES-KOH (pH 7.0) and 5 mM EDTA. Derivatization with MBB (73.7 μM final concentration) was carried out at 70°C for 3 min. HPLC analyses were performed on a Zorbax C-18 column (Hewlett Packard) and Shimadzu LC-10Ai HPLC system with RF-10AXL fluorescence detector. The fluorescence of MBB derivatized thiols was detected at 380 nm excitation and 490 nm emission wavelengths. Mobile phase A contained 0.25% (w/v) d-camphorsulphonate in water, pH 2.7. Mobile phase B contained 0.25% (w/v) d-camphorsulphonate and 25% isopropanol.

Three peaks were detected in all samples (Fig. 5). By comparison to standards and Δ*gshA* cells, the major peak of the WT cells is GSH. The early 52 min peak was present in the control sample containing dye alone and likely to be a contaminant (data not shown). The third peak (70 min) contained an unidentified thiol compound, which is also present in Δ*gshA* cells and thus, does not originate from GSH. In addition, all cells contained small variable amounts of the fourth minor peak, which by its mobility could correspond to GSP (85 min).

The GSSG reductase recycling assay was used to determine the total GSH+GSSG and GSSG only concentrations *in vivo* and in culture supernatants (Anderson, 1985). Approximately 1×10^9 cells growing in LB or M9 medium were re-suspended in 20 μl of buffer containing 143 mM sodium phosphate (pH 7.4) and 6.3 mM EDTA and 10 μl of 10% 5-sulphosalicylic acid. Samples were centrifuged at 15 700 *g* for 5 min to remove protein precipitates. For each reaction, 210 μl of 0.25 mg ml^{-1} NADPH (Sigma) and 30 μl of 6 mM 5,5′-dithiobis(2-nitrobenzoic acid) (DTNB, Sigma) were mixed together and incubated at 30°C for 15 min. The reaction was started by addition of 60 μl of sample and 3 μl of 266 U ml^{-1} yeast glutathione reductase enzyme (Sigma). For GSSG measurements, 20 μl of each sample was treated with 0.4 μl of 2-vinylpyridine. The pH of sample was adjusted to 6–7 by triethanolamine. The rate of absorbance increase at 412 nm was monitored for 5 min. The assay was calibrated with GSH and GSSG standards (Sigma), in the range of 0.15–1.2 nmol. The same reactions were set to measure GSH and GSSG in culture supernatants, except 25 μl of each supernatant was used in the reaction.

Phase-contrast and fluorescence microscopy

For phase-contrast microscopy, *E. coli* strains were grown overnight in LB medium and diluted 1:100 into fresh M9 medium and grown at 37°C for 20 h. One microlitre of culture was spread onto the slide and a coverslip was placed on the top. The slides were viewed and photographed with Spot (Insight) camera mounted onto an Olympus BX50 microscope.

The LIVE/DEAD BacLight Bacterial Viability kit (Invitrogen) was used to score live and dead cells. Samples were processed and stained as recommended by the manufacturer.

Acknowledgements

This work was supported by the National Institutes of Health Grant 2RO1-AI052293 to H.I.Z.

References

Andersen, C., Hughes, C., and Koronakis, V. (2001) Protein export and drug efflux through bacterial channel-tunnels. *Curr Opin Cell Biol* **13:** 412–416.

Anderson, M.E. (1985) Determination of glutathione and glutathione disulfide in biological samples. *Methods Enzymol* **113:** 548–555.

Bleuel, C., Grosse, C., Taudte, N., Scherer, J., Wesenberg, D., Krauss, G.J., *et al*. (2005) TolC Is involved in enterobactin efflux across the outer membrane of *Escherichia coli*. *J Bacteriol* **187:** 6701–6707.

Bollinger, J.M., Jr, Kwon, D.S., Huisman, G.W., Kolter, R., and Walsh, C.T. (1995) Glutathionylspermidine metabolism in *Escherichia coli*. Purification, cloning, overproduction, and characterization of a bifunctional glutathionylspermidine synthetase/amidase. *J Biol Chem* **270:** 14031–14041.

Brumaghim, J.L., Li, Y., Henle, E., and Linn, S. (2003) Effects of hydrogen peroxide upon nicotinamide nucleotide metabolism in *Escherichia coli*: changes in enzyme levels and nicotinamide nucleotide pools and studies of the oxidation of NAD(P)H by Fe(III). *J Biol Chem* **278:** 42495–42504.

Cosme, A.M., Becker, A., Santos, M.R., Sharypova, L.A., Santos, P.M., and Moreira, L.M. (2008) The outer membrane protein TolC from *Sinorhizobium meliloti* affects protein secretion, polysaccharide biosynthesis, antimicrobial resistance, and symbiosis. *Mol Plant Microbe Interact* **21:** 947–957.

Dancey, G.F., Levine, A.E., and Shapiro, B.M. (1976) The NADH dehydrogenase of the respiratory chain of *Escherichia coli*. I. Properties of the membrane-bound enzyme, its solubilization, and purification to near homogeneity. *J Biol Chem* **251:** 5911–5920.

Datsenko, K.A., and Wanner, B.L. (2000) One-step inactivation of chromosomal genes in *Escherichia coli* K-12 using PCR products. *Proc Natl Acad Sci USA* **97:** 6640–6645.

Dukan, S., and Nystrom, T. (1999) Oxidative stress defense and deterioration of growth-arrested *Escherichia coli* cells. *J Biol Chem* **274:** 26027–26032.

Fairlamb, A.H., Henderson, G.B., and Cerami, A. (1986) The biosynthesis of trypanothione and N1-glutathionylspermidine in *Crithidia fasciculata*. *Mol Biochem Parasitol* **21:** 247–257.

Ferhat, M., Atlan, D., Vianney, A., Lazzaroni, J.C., Doublet, P., and Gilbert, C. (2009) The TolC protein of *Legionella pneumophila* plays a major role in multi-drug resistance and the early steps of host invasion. *PLoS ONE* **4:** e7732.

Fuchs, J.A. (1995) Glutathione mutants. *Methods Enzymol* **252:** 83–92.

Gennis, R.B., and Stewart, V. (1996) Respiration. In Escherichia coli *and* Salmonella*: Cellular and Molecular Biology*. Neidhardt, F.C., Curtiss, R., III, Ingraham, J.L., Lin, E.C.C., Low, K.B., Magasanik, B., *et al*. (eds)., 2nd ed. Washington, DC: American Society for Microbiology, pp. 217–261.

Gilson, L., Mahanty, H.K., and Kolter, R. (1990) Genetic analysis of an MDR-like export system: the secretion of colicin V. *EMBO J* **9:** 3875–3894.

Helbig, K., Bleuel, C., Krauss, G.J., and Nies, D.H. (2008) Glutathione and transition-metal homeostasis in *Escherichia coli*. *J Bacteriol* **190:** 5431–5438.

Holland, I.B., Blight, M.A., and Kenny, B. (1990) The mechanism of secretion of hemolysin and other polypeptides from gram-negative bacteria. *J Bioenerg Biomembr* **22:** 473–491.

Imlay, J.A., and Linn, S. (1988) DNA damage and oxygen radical toxicity. *Science* **240:** 1302–1309.

Kleerebezem, M., Crielaard, W., and Tommassen, J. (1996) Involvement of stress protein PspA (phage shock protein A) of *Escherichia coli* in maintenance of the protonmotive force under stress conditions. *EMBO J* **15:** 162–171.

Kobayashi, R., Suzuki, T., and Yoshida, M. (2007) *Escherichia coli* phage-shock protein A (PspA) binds to membrane phospholipids and repairs proton leakage of the damaged membranes. *Mol Microbiol* **66:** 100–109.

Leonardo, M.R., Dailly, Y., and Clark, D.P. (1996) Role of NAD in regulating the adhE gene of *Escherichia coli*. *J Bacteriol* **178:** 6013–6018.

Matsumura, H., and Miyachi, S. (1980) Cycling assay for nicotinamide adenine dinucleotides. *Methods Enzymol* **69:** 465–470.

Nystrom, T. (2004) Stationary-phase physiology. *Annu Rev Microbiol* **58:** 161–181.

Osborn, M.J., Gander, J.E., Parisi, E., and Carson, J. (1972) Mechanism of assembly of the outer membrane of *Salmonella typhimurium*. *J Biol Chem* **247:** 3962–3972.

Pai, C.H., Chiang, B.Y., Ko, T.P., Chou, C.C., Chong, C.M., Yen, F.J., *et al*. (2006) Dual binding sites for translocation catalysis by *Escherichia coli* glutathionylspermidine synthetase. *EMBO J* **25:** 5970–5982.

Platz, G.J., Bublitz, D.C., Mena, P., Benach, J.L., Furie, M.B., and Thanassi, D.G. (2009) A tolC mutant of *Francisella tularensis* is hypercytotoxic and elicits increased proinflammatory responses from host cells. *Infect Immun* **78:** 1022–1031.

Pruss, B.M., Nelms, J.M., Park, C., and Wolfe, A.J. (1994) Mutations in NADH:ubiquinone oxidoreductase of *Escherichia coli* affect growth on mixed amino acids. *J Bacteriol* **176:** 2143–2150.

Rosner, J.L., and Martin, R.G. (2009) An excretory function for the *Escherichia coli* outer membrane pore TolC: upregulation of *marA* and *soxS* transcription and Rob activity due to metabolites accumulated in *tolC* mutants. *J Bacteriol* **191:** 5283–5292.

Smith, K., Borges, A., Ariyanayagam, M.R., and Fairlamb, A.H. (1995) Glutathionylspermidine metabolism in *Escherichia coli*. *Biochem J* **312:** 465–469.

Tabor, H., and Tabor, C.W. (1975) Isolation, characterization, and turnover of glutathionylspermidine from *Escherichia coli*. *J Biol Chem* **250:** 2648–2654.

Tabor, C.W., Tabor, H., and Hafner, E.W. (1978) *Escherichia coli* mutants completely deficient in adenosylmethionine decarboxylase and in spermidine biosynthesis. *J Biol Chem* **253:** 3671–3676.

Tatsumi, R., and Wachi, M. (2008) TolC-dependent exclusion of porphyrins in *Escherichia coli*. *J Bacteriol* **190:** 6228–6233.

Thanabalu, T., Koronakis, E., Hughes, C., and Koronakis, V. (1998) Substrate-induced assembly of a contiguous channel for protein export from *E. coli*: reversible bridging of an inner-membrane translocase to an outer membrane exit pore. *EMBO J* **17:** 6487–6496.

Tikhonova, E.B., and Zgurskaya, H.I. (2004) AcrA, AcrB, and TolC of *Escherichia coli* form a stable intermembrane multidrug efflux complex. *J Biol Chem* **279:** 32116–32124.

Tikhonova, E.B., Wang, Q., and Zgurskaya, H.I. (2002) Chimeric analysis of the multicomponent multidrug efflux transporters from gram-negative bacteria. *J Bacteriol* **184:** 6499–6507.

Tikhonova, E.B., Dastidar, V., Rybenkov, V.V., and Zgurskaya, H.I. (2009) Kinetic control of TolC recruitment by multidrug efflux complexes. *Proc Natl Acad Sci USA* **106:** 16416–16421.

Touze, T., Eswaran, J., Bokma, E., Koronakis, E., Hughes, C., and Koronakis, V. (2004) Interactions underlying assembly of the *Escherichia coli* AcrAB–TolC multidrug efflux system. *Mol Microbiol* **53:** 697–706.

Webber, M.A., Bailey, A.M., Blair, J.M., Morgan, E., Stevens, M.P., Hinton, J.C., *et al*. (2009) The global consequence of disruption of the AcrAB–TolC efflux pump in *Salmonella enterica* includes reduced expression of SPI-1 and other attributes required to infect the host. *J Bacteriol* **191:** 4276–4285.

Wiriyathanawudhiwong, N., Ohtsu, I., Li, Z.D., Mori, H., and Takagi, H. (2009) The outer membrane TolC is involved in cysteine tolerance and overproduction in *Escherichia coli*. *Appl Microbiol Biotechnol* **81:** 903–913.

Xie, Q.W., Tabor, C.W., and Tabor, H. (1993) Deletion mutations in the *speED* operon: spermidine is not essential for the growth of *Escherichia coli*. *Gene* **126:** 115–117.

Yamanaka, H., Kobayashi, H., Takahashi, E., and Okamoto, K. (2008) MacAB is involved in the secretion of *Escherichia coli* heat-stable enterotoxin II. *J Bacteriol* **190:** 7693–7698.

Yun, N.-R., San, K.-Y., and Bennett, G.N. (2005) Enhancement of lactate and succinate formation in *adhE* or *pta-ackA* mutants of NADH dehydrogenase-deficient *Escherichia coli*. *J Appl Microbiol* **99:** 1404–1412.

Zgurskaya, H.I. (2009) Multicomponent drug efflux complexes: architecture and mechanism of assembly. *Future Microbiol* **4:** 919–932.